

Synthesis and swelling behavior of xanthan-based hydrogels

Vania Blasques Bueno, Ricardo Bentini, Luiz Henrique Catalani, Denise Freitas Siqueira Petri*

Instituto de Química, Universidade de São Paulo, P.O. Box 26077, São Paulo, SP 05513-970, Brazil

ARTICLE INFO

Article history:

Received 1 August 2012

Received in revised form

12 September 2012

Accepted 23 October 2012

Available online 1 November 2012

Keywords:

Hydrogels

Xanthan

Citric acid crosslinking

Swelling

Water diffusion

Tensiometry

ABSTRACT

In this work xanthan chains were crosslinked by esterification reaction at 165 °C either in the absence or in the presence of citric acid. Higher crosslinking density was obtained using citric acid, as evidenced by its lower swelling degree. Tensiometry, a very precise and sensitive technique, was applied to study swelling rates and diffusion mechanisms of water, which was initially quasi-Fickian, controlled by wicking properties, changing to Fickian or Anomalous, depending on hydrogel composition. Hydrogels swelling degree increased at high pH values, due to electrostatic repulsion and ester linkages rupture. Equilibrium swelling degree was affected by salts, depending on gel composition and kind of salt. Effects could be explained by interaction between ions and polymeric chains, EPA/EPD ability of water or osmotic gradient.

© 2012 Elsevier Ltd. All rights reserved.

1. Introduction

Xanthan gum is a high molecular weight polysaccharide with branched chains and acidic characteristic produced predominantly by *Xanthomonas campestris* (Dumitriu, 2005) in aerobic conditions from sugar cane, corn or their derivatives and is largely used as thickener agent in food, cosmetics and drilling fluids (Geremia & Rinaudo, 2005). It consists of D-glucosyl, D-mannosyl, and D-glucuronyl acid residues in a 2:2:1 molar ratio and variable proportions of O-acetyl and pyruvyl residues. Trisaccharide side-chains are composed of mannose (β -1,4) glucuronic acid (β -1,2) mannose attached to alternate glucose residues in the backbone by α -1,3 linkages. A ketal linkage joined by a pyruvic acid moiety is on approximately half of the terminal mannose residues. Acetyl groups are often present as 6-O substituents on the internal mannose residues. Under low ionic strength or high temperature xanthan chains appear as disordered and flexible structures (Dumitriu, 2005; Tinland & Rinaudo, 1989), whereas at low temperature or high ionic strength they present ordered structures (single or double helix conformations) (Dumitriu, 2005). At pH > ~4.5 O-acetyl and pyruvyl residues are deprotonated, increasing charge density along the xanthan chains and enabling their physical crosslinking mediated by Ca²⁺ ions (Bergmann, Furth, & Mayer, 2008; Dário, Hortêncio, Sierakowski, Queiroz Neto, & Petri, 2011). Alternatively, xanthan can be crosslinked by using adipic acid dihydrazide

(Bejenariu, Popa, Picton, & Le Cerf, 2009) or sodium trimetaphosphate (STMP) (Bejenariu, Popa, Dulong, Picton, & Le Cerf, 2009).

Hydrogels are tridimensional networks of hydrophilic polymers, which are able to swell in water (Peppas, 1986). Their ability to respond to external stimuli as temperature (Kacmaz & Gurdag, 2006), pH (Thakur, Wanchoo, & Singh, 2011), ionic strength (Lai & Li, 2010), electric or magnetic fields depends on the nature of polymer chains and makes them useful in applications such as controlled drug delivery (Mudassir, Ranjha, & Sheikh, 2011; Pal, Banthia, & Majundar, 2009), separation/concentration process (Fredolini et al., 2008) or agricultural applications (Rudzinski et al., 2002).

Polysaccharide biocompatibility, abundance in nature (da Cunha, de Paula, & Feitosa, 2009) and hydrogels similarity with biological systems are characteristics of a material of great interest, mainly on biomedical applications (Geckil, Xu, Zhang, Moon, & Demirci, 2010; Pal et al., 2009). Some polysaccharide-based hydrogels, e.g. from chitosan, are highly explored on literature (Muzzarelli, 2009). Especially, stimuli-responsive polysaccharides hydrogels, as, for example, chitosan and dextran hydrogels, whose swelling degree is sensitive to pH, exhibit smart hydrogels characteristics (a smart or stimuli-responsive hydrogel is the one that presents abrupt changes on its physical network nature as response to external or internal stimuli, for example: changes in temperature, pH, ionic strength, electric current) (Soppimath, Aminabhavi, Dave, Kumbar, & Rudzinski, 2002). These hydrogels are interesting for applications involving controlled drug delivery (Soppimath et al., 2002; Zuidema, Pap, Jaroch, Morrison, & Gilbert, 2011).

* Corresponding author. Tel.: +55 11 30913831; fax: +55 11 38155579.

E-mail addresses: dfsp@iq.usp.br, dfsp@usp.br (D.F.S. Petri).

Understanding the swelling behavior of hydrogels in the presence of ions is important from the practical and theoretical points of view. The effects of Hofmeister ions on the colloidal behavior were originally attributed to perturbations of bulk water properties and macromolecule hydration, related to electron-pair acceptance – EPA – and electron-pair donation – EPD – ability of water, which can be respectively enhanced by hydration to cations and anions (Muta, Kojima, Kawauchi, Tachibana, & Satoh, 2001a, 2001b). Cations with a very small radius or a large charge density have more influence on EPA of water, increasing its ability to hydrate electron donor groups, as carbonyls, for example, causing “salting in” or swelling effect, as observed for poly(N-vinyl-2-pyrrolidone) hydrogels, where Ca^{2+} , Mg^{2+} and Li^{+} increased swelling degree, whereas K^{+} , Na^{+} and Cs^{+} caused hydrogel shrinking (Bueno, Cuccovia, Chaimovich, & Catalani, 2009; Takano, Ogata, Kawauchi, Satoh, & Komiyama, 1998). However, nowadays there are evidence that such effects might be due to specific interactions between ions and macromolecules and their first hydration shell (Blachechen, Silva, Barbosa, Itri, & Petri, 2012; Cacace, Landau, & Ramsden, 1997; Kunz, Lo Nostro, & Ninham, 2004; Leontidis, 2002; Zhang & Cremer, 2006), which involve the relative polarizabilities of the ions (Zhang, Furry, Bergbreiter, & Cremer, 2005) and changes in the Hamaker constant for particle–particle interaction and in the ion hydration layer (Manciu & Ruckenstein, 2007; Petrache, Zemb, Belloni, & Parsegian, 2006; Santos & Levin, 2011), affecting the colloidal behavior. Ions were ordered in the so-called Hofmeister’s series, where ions that destabilize folded proteins and cause “salting-in” effect are called chaotropes or “water structure breakers” ions; SCN^{-} and Ba^{2+} ions are the most chaotrope ones of the series. Chaotropes are usually large and present high polarizabilities. Consequently, they have weak electric fields, losing their hydration layer easily. In contrast, ions which tend to stabilize proteins and cause “salting-out” effects are called kosmotropes or “water structure makers”; citrate and $(\text{CH}_3)_4\text{N}^{+}$ ions are the most kosmotropes of the series. Usually kosmotropes are small and present low polarizabilities. Since they have high electric fields at short distances, they do not lose their hydration layer easily.

Gel swelling might be also affected by the osmotic effect, which drives water molecules out the hydrogel structure, causing gel shrinking. Such effect was observed for PNIPAM microparticles, where the addition of non-crosslinked polymer to hydrogel suspension provided a concentration gradient, as the free polymer chain was not able to permeate the microgel. The gradient was compensated by gel deswelling, balancing chemical potentials inside and outside of the network (Saunders & Vincent, 1999). Ions are totally excluded from intermediate and bounded water due to entropic factors and their transport inside gel structure occurs only in the bulk phase (Wisniewski & Kim, 1980), causing an ionic concentration gradient inside the gel structure. This gradient shifts the intermediate water and bound water to bulk, to promote osmotic system stabilization. Thus, polymer chains dehydration and consequent increase of hydrophobic interactions among them lead to gel shrinking (see cartoon on [Supplementary material 3](#)).

In this work, xanthan hydrogels were obtained either in the absence or in the presence of citric acid, a non-toxic crosslinker for polysaccharides (Reddy & Yang, 2010; Yang, Wang, & Kang, 1997). Xanthan hydrogels were characterized by gel content and scanning electron microscopy (SEM). Their swelling behavior was investigated under different medium characteristics, as salt type (Hofmeister series) and pH, in order to evaluate their responsive characteristics. Moreover, tensiometry, a very precise and sensitive technique, was applied to study swelling rates and diffusion mechanisms of water. To the best of our knowledge, it is the first time that tensiometry was used for the determination of diffusion mechanism of water in hydrogels.

2. Experimental

2.1. Materials

Commercial xanthan (Kelzan[®], CP Kelco, USA, degree of pyruvate = 0.38, degree of acetyl = 0.41, $M_v \sim 1.0 \times 10^6$ g/mol, degree of polymerization ~ 1072) was used as received. Citric acid (Analitica Química, Brazil) was recrystallized twice from water before use. NaCl and HCl were obtained from Casa Americana – Brazil. KCl and NH_4Cl were obtained from Nuclear – Casa da Química, Brazil. NaF, NaSCN, LiCl, *n*-hexane and NaOH were obtained from Synth. All these reagents are analytical grade and were used without further purification. Salts were dried in a desiccator containing silica-gel under vacuum prior to use. Deionized water was used in all experiments.

2.2. Xanthan hydrogels preparation

Xanthan-based hydrogels were prepared as follows: xanthan films were produced by casting a 6 g L^{-1} xanthan aqueous solution in the absence or in the presence of citric acid at 0.3 g L^{-1} . This concentration of citric acid was chosen because it worked well for starch crosslink (Reddy & Yang, 2010). The solutions were homogenized with an Ika Turrax[®] stirrer at 18,000 rpm for 3 min and submitted to centrifugation for 5 min at 3600 rpm, to remove air bubbles prior to casting. Crosslinking was achieved by heating the dried films (~ 0.02 mm thick) at 165°C for 7 min. The sol fraction was extracted with water at $\sim 70^\circ\text{C}$, under gentle magnetic stirring, during 24 h. The resulting xanthan hydrogels (XNT hydrogel) and xanthan–citric acid hydrogels (XCA hydrogel) were dried at 45°C for 48 h.

2.3. Xanthan-based hydrogels characterization

Gel content and swelling degree at equilibrium (Q) were calculated according to Eqs. (1) and (2), respectively:

$$\text{Gel content (\%)} = \left[1 - \left(\frac{m_{\text{pol}} - m_{\text{driedgel}}}{m_{\text{pol}}} \right) \right] \times 100 \quad (1)$$

$$Q = \frac{m_{\text{water}}}{m_{\text{driedgel}}} = \frac{m_{\text{swollengel}} - m_{\text{driedgel}}}{m_{\text{driedgel}}} \quad (2)$$

where m_{pol} is the initial mass of polymer, m_{driedgel} is the mass of dried hydrogel, m_{water} is the amount of water absorbed by the gel and $m_{\text{swollengel}}$ is the mass of swollen hydrogel.

SEM analysis was performed in a Jeol microscope FEG7401F equipped with a Field-Emission Gun. Samples were prepared by cryo-fracturing freeze-dried hydrogels. Resultant surfaces were analyzed after gold coating (sputtering). Fourier transform infrared spectroscopy was performed with BOMEM MB 100 equipment using KBr pellets. Mechanical properties were investigated in a DMA Q800 from TA Instruments. Analyses were performed for dried films about 0.010 mm thick with rectangular dimensions ($\sim 30 \text{ mm} \times 6 \text{ mm}$).

Hydrogel swelling rate was determined with a Krüss K100 precision tensiometer (Krüss, Hamburg Germany), in the sorption mode, at 25°C (see [Supplementary material 1](#)). Freeze-dried hydrogel samples were cut with scalpel in rectangles ($5 \text{ mm} \times 20 \text{ mm}$) and suspended in an arrangement of Nylon[®] wires trapped with a clamp model SH0602. Freeze-dried XNT and XCA hydrogels were ~ 0.06 mm and ~ 0.03 mm thick, respectively. A vessel with water, placed on a platform moved until water touched the sample. Water uptake occurred due to capillary forces. Mass variation due to water sorption or hydrogel swelling was automatically recorded as a function of time for at least three different samples of same material in order to determine mean Q values (Eq. (2)) with standard deviation

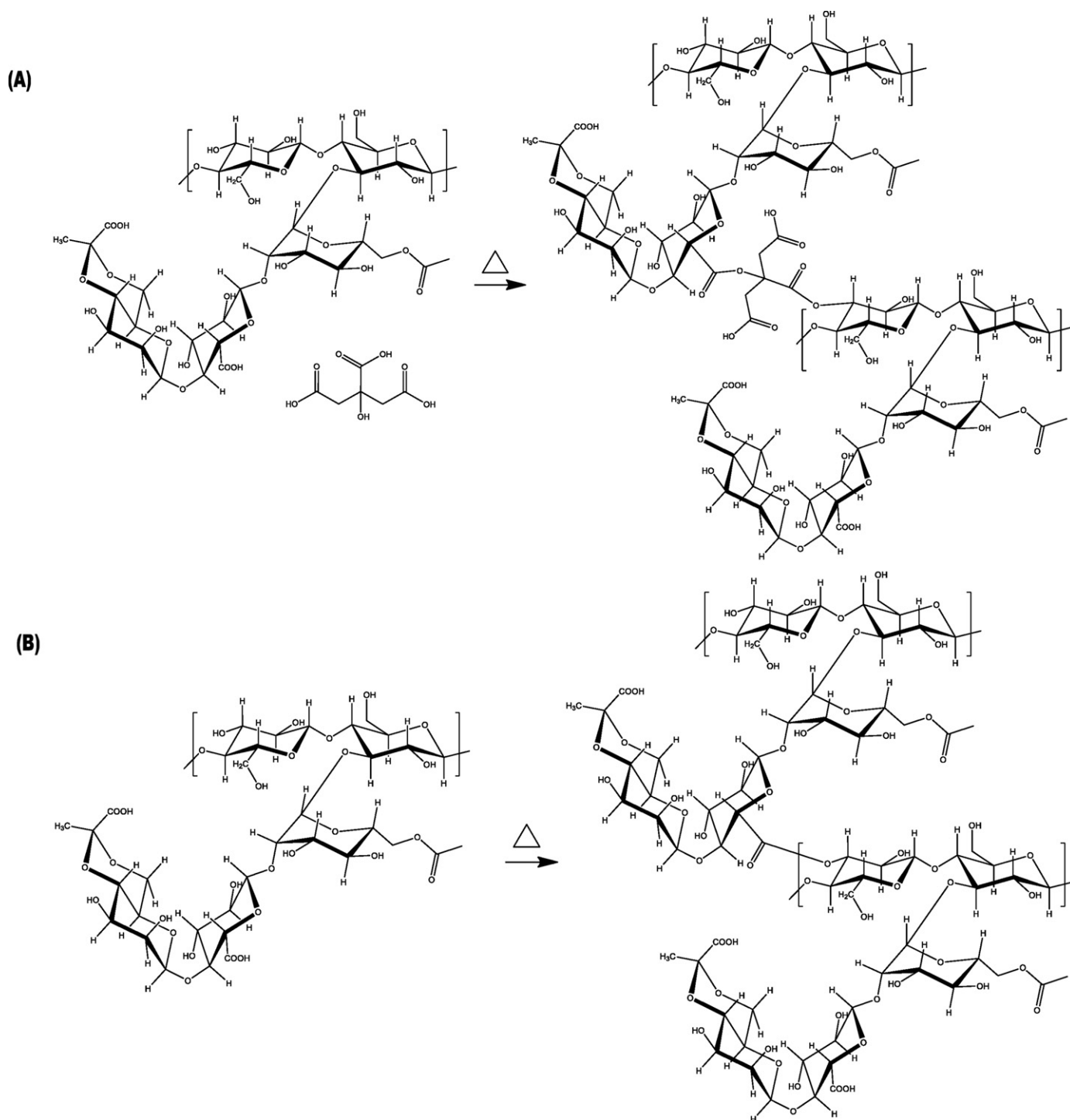


Fig. 1. Scheme of (A) xanthan crosslinking reaction with citric acid and (B) xanthan crosslinking reaction (dehydration).

of 13%. In a similar way *n*-hexane sorption was measured in the tensiometer, using the clamp directly to fix the freeze-dried samples (10 mm × 10 mm).

The diffusion mechanism of small molecules through a gel structure is classified according to the diffusional coefficient, *n*, value, which can be calculated according to Eq. (3) (Peppas, 1986).

$$\frac{M_t}{M_e} = kt^n \quad (3)$$

where *M_t* and *M_e* are the masses of water absorbed at a given time *t* and at equilibrium condition, respectively, *k* is a constant and *n* is

the diffusional coefficient. The linear coefficient of $\ln(M_t/M_e)$ as a function of $\ln(t)$ corresponds to *n*.

In order to study media effects on hydrogels swelling experiments were done as follows: hydrogels, totally swollen in water, were immersed into different solutions (HCl 0.1 mol L⁻¹, NaOH 0.1 mol L⁻¹, or LiCl, KCl, NaCl, NaSCN and NaF 1.0 mol L⁻¹ solutions). After 24 h, hydrogels were removed from the medium and weighed. Relative swelling ratio *Q/Q₀* was calculated as Eq. (4):

$$\frac{Q}{Q_0} = \frac{Q_{\text{solution}}}{Q_{\text{water}}} \quad (4)$$

where Q_{solution} is the swelling degree of hydrogel in the chosen solution and Q_{water} is the swelling degree of the same hydrogel sample in pure water.

3. Results and discussion

3.1. Xanthan crosslinking

Xanthan crosslinking by citric acid took place at 165 °C by a condensation process, which involved dehydration and ester linkages formation between them (Reddy & Yang, 2010; Yang et al., 1997). Xanthan chains are thermally stable at this temperature, as evidenced by thermal gravimetric analysis (Supplementary material 4). In general, such chemical bonds create a tridimensional hydrophilic structure that characterizes a chemical hydrogel (Hoffman, 2002), as schematically presented in Fig. 1A. In the absence of citric acid the intra- and intermolecular ester bonds are due to xanthan chains dehydration and trans-esterification reactions, as represented in Fig. 1B.

In the absence of citric acid, esterification between xanthan acid groups (pyruvyl or acetyl) and OH groups can also occur upon heating the xanthan film. Such crosslinking reaction can be evidenced by FTIR spectroscopy (see Supplementary material 2). Carbonyl bands of xanthan corresponding to the acidic and ester forms can be observed at 1643 cm⁻¹ and 1728 cm⁻¹, respectively. The sol fraction of crosslinked xanthan sample was removed prior to FTIR analysis. The relative intensities in the carbonyl range changed; after band deconvolution, acid/ester areas ratio decreased from 7 to 4, indicating conversion of the acid to the ester by heating. In the presence of citric acid it was not observed significant changes on carbonyls intensities ratio (acid/ester areas ratio decrease from 2.4 to 2.0). This is due to crosslinker addition, which balances carbonyls amounts.

Crosslinking density is inversely proportional to swelling capacity (Peppas, 1986). Table 1 shows that XNT samples presented lower gel content and higher swelling degree (Q) than XCA samples and other xanthan based gels reported in the literature (Bejenariu, Popa, Picton, et al., 2009; Bejenariu, Popa, Dulong, et al., 2009; Shalviri, Liu, Abdekhoodaie, & Wu, 2010), because no crosslinker was added and pure xanthan chains have limited number of groups that can be crosslinked. On the other hand, gel content and Q values found for XCA are comparable to those prepared with dihydrazide (Bejenariu, Popa, Picton, et al., 2009) or STMP (Bejenariu, Popa, Dulong, et al., 2009), due to crosslinker addition.

SEM analysis of cryofracture surface shows that XNT hydrogels (Fig. 2A) present heterogeneous porous structure and nanofibrils (about 20–30 nm diameter), which can be related to low crosslinking density. XCA hydrogels present more homogeneous porous structure and practically no nanofibrils (Fig. 2B), indicating that citric acid is an efficient cross-linking agent. These morphological features corroborated with the gel content and Q values in Table 1.

Young's modulus, stress at break (σ) and elongation at break (ϵ) values determined for XNT and XCA dried gels were smaller than those measured for uncrosslinked xanthan chains (Table 1). The differences in the mechanical properties are probably due to the different packing densities in each sample. Irregular crosslinking points induce spaces formation between xanthan chains. Such spaces decrease the packing density, decreasing Young's modulus, σ and ϵ values. The density of uncrosslinked xanthan films was determined as 1.8 g cm⁻³, whereas XNT and XCA collapsed films presented density values of 0.60 and 0.62 g cm⁻³, respectively. XCA is slightly more rigid than XNT, due to the higher crosslinking homogeneity. The hydrogels properties of XCA are comparable to those reported for xanthan–starch films (Veiga-Santos, Oliveira, Cereda, Alves, & Scamparini, 2005).

3.2. Solvents diffusional mechanism and swelling rates

The study of transport of molecules, as the swelling behavior in different media compositions, is important in the understanding of delivery systems in biomedicine (Pal et al., 2009) and agriculture applications (Rudzinski et al., 2002). Solvent and solute transport through a polymeric network can be described by different mechanisms, all of them are based on the diffusional coefficient n (see Eq. (3)). Fickian diffusion or Case I Diffusion mechanism describes the transport of molecules through matrix without any specific interactions between liquid molecule and matrix, where the typical n value is 0.5. Oppositely, Case II Diffusion considers interaction between penetrant molecule and polymer matrix, when n value is 1.0 (Hansen, 2010; Thomas & Windle, 1982). Anomalous Diffusion mechanism is intermediate between Fickian and Case II Diffusion mechanisms with $0.5 < n < 1.0$. In the Super-Case II Diffusion ($n > 1.0$), transport increase is faster than in the Case II Diffusion (Hansen, 2010). Quasi-Fickian diffusion describes a stereoselective transport of the molecule in the matrix (Londhe, Gattani, & Surana, 2010; Solinis et al., 2002) typically presents $n < 0.5$.

The initial step in the swelling process might reveal important information about the gel porous structure (Galet, Patry, & Dodds, 2010). However, it is difficult to measure because in some cases it is a very fast process. In the present study a high precision tensiometer was used to overcome this drawback, because this technique allows measuring mass variation due to solvent absorption in a very short time interval with precision and high sensibility, enabling observation of swelling events at its initial step. To the best of our knowledge, this is the first time this technique has being used to evaluate hydrogels swelling mechanisms.

The diffusion mechanism of n -hexane and water in XNT and XCA samples was investigated by recording the normalized mass sorption as a function of time (Eq. (3)), using freeze-dried samples which were stored in a desiccator over silica gel until the moment of experiment. The linearization yields the n value, which characterizes the type of diffusion mechanism. n -Hexane was chosen because it wets the polymer matrix (its low surface energy of 18.4 mN m⁻¹ contributes to high spreading and low contact angle, $\theta \sim 0^\circ$), but without swelling.

Fig. 3A shows the normalized n -hexane mass sorption as a function of time. From curve linearization (Fig. 3B) the n values 0.05 and 0.11 were calculated for XCA and XNT, respectively, indicating a quasi-Fickian diffusion mechanism, where n -hexane molecules are supposed to pass through a preferential way inside interconnected pores, guided by wicking, which is the spontaneous absorption of a liquid by the action of capillary pressure (Masoodi & Pillai, 2010).

Fig. 3E shows the swelling curves in water for xanthan hydrogel samples. Fig. 3C and D shows the dependence of $\ln(M_t/M_e)$ on $\ln(t)$ in two regions (beginning and final of water sorption curve) for swelling in water of XNT and XCA networks, respectively, with their respective n values. Diffusional coefficient on the initial swelling for both hydrogels was calculated as 0.33 and 0.37 for XNT and XCA hydrogels, respectively (Fig. 3C), characterizing a quasi-Fickian diffusion mechanism without relaxation of polymeric chains, referred to preferential passage of water by interconnected pores, as observed for n -hexane.

After this initial water sorption, water uptake by XNT hydrogels (swelling) follows the Fickian diffusion Mechanism (calculated n value is 0.51 – Fig. 3D). Another example of water Fickian diffusion by a hydrogel is the water uptake by cylinders of crosslinked poly(HEMA) (Hill, Lim, & Whittaker, 1999). In this diffusion model, it is assumed that there is no interaction between network and transported molecule (Hill et al., 1999). As crosslinking density is lower in this gel, swelling degree is larger due to higher bulk water contents, justifying Fickian mechanism.

Table 1

Gel content, swelling degree Q , Young's modulus (E), stress at break (σ) and elongation at break (ε) measured for uncrosslinked xanthan, dried XNT and XCA hydrogels and literature data (Bejenariu, Popa, Picton, et al., 2009; Bejenariu, Popa, Dulong, et al., 2009; Shalviri et al., 2010).

	Uncrosslinked xanthan	XNT hydrogel	XCA hydrogel	Xanthan-dihydrazide hydrogel	Xanthan-STMP hydrogel	Xanthan-starch hydrogel
Gel content (%)	–	20 ± 5	75 ± 15	70	50	–
Q	–	150 ± 10	27 ± 3	10–50	30–60	2–7
E (GPa)	3.1 ± 0.5	1.1 ± 0.1	1.9 ± 0.8	–	–	–
σ (MPa)	40 ± 4	14 ± 4	18 ± 5	–	–	–
ε (%)	3 ± 2	0.2 ± 0.1	0.10 ± 0.05	–	–	~5 ^a

^a Veiga-Santos et al. (2005).

The n values calculated for XCA hydrogels was ~0.8 (Fig. 3D), which is typical of Anomalous Diffusion Mechanism. In this case, as crosslinking density is large, the free volume (bulk water) is small, decreasing the diffusion rate (Hill et al., 1999; Krongauz, 2010; Wu, Joseph, & Aluru, 2009). Some authors say that this water has supercooled liquid phase characteristics (Wu et al., 2009). Similar behavior was observed for hydrogels based on polyacrylamide and methylcellulose polysaccharide (Aouada, Moura, Silva, Muniz, & Mattoso, 2011), where variations in the gel formulation changed the diffusion mechanism from Fickian to Anomalous.

A significant amount of water in a hydrogel is bulk water, which does not differ significantly from bulk water out of the gel. However, bulk water is not the only water structure present in hydrogels. Studies involving other water-absorbent polymeric systems suggest that there are, at least, three kinds of water structure in these systems: bulk water, intermediate water and total bound-water (primary bound-water and secondary bound-water) (Gulrez, Al-Assaf, & Phillips, 2011; Wisniewski & Kim, 1980). According to Gulrez et al. (2011), when hydrogels are exposed to water, the first kind of water that will be present is the primary bound-water, related to hydration of hydrophilic groups of the polymer.

This first bound-water is very difficult to remove from the gel. Hydrophilic groups' hydration starts the swelling of the polymer, exposing hydrophobic groups, which interacts with water forming the secondary bound-water. After this, intermediate and bulk water will be present due to osmotic driving force that forces hydrogel to infinite dilution and is opposite to crosslinks (elastic network retraction force). Water sorption curves obtained for XNT and XCA (Fig. 3E) show different stages, which can be related to the different hydration water layers. The first event, as described for n -hexane, is guided by hydrogel wicking (capillarity).

3.3. Equilibrium swelling dependence on media characteristics

Swelling of hydrogels can be influenced by the medium pH (Thakur et al., 2011), especially when there are ionizable groups present in their structure. For instance, at pH > 4 the carboxylic acid groups in poly(acrylic acid) (Muta, Kawauchi, & Satoh, 2003) and poly(acrylamide-co-acrylate) (Candido et al., 2012) start to deprotonate, favoring the polymer–polymer repulsion and the interaction with water. XNT and XCA hydrogels have acidic groups from *O*-acetyl and pyruvyl residues or from citric acid (in XCA

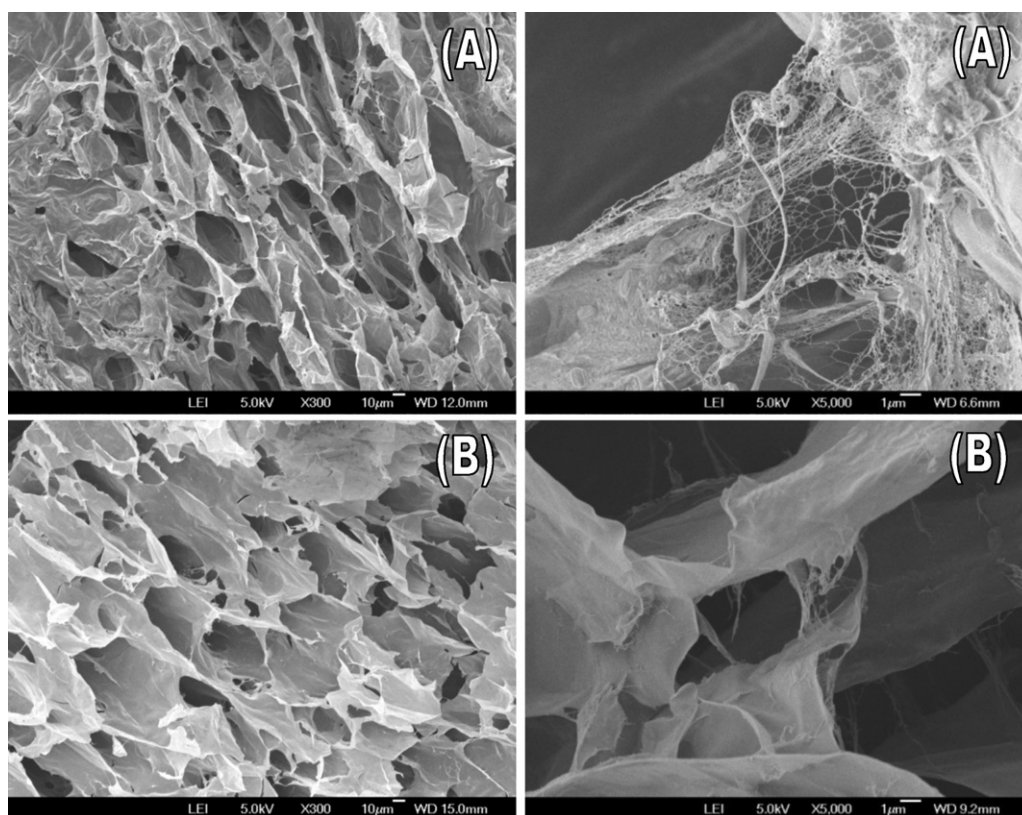


Fig. 2. SEM images obtained for (A) XNT and (B) XCA hydrogels, each one in two different magnifications.

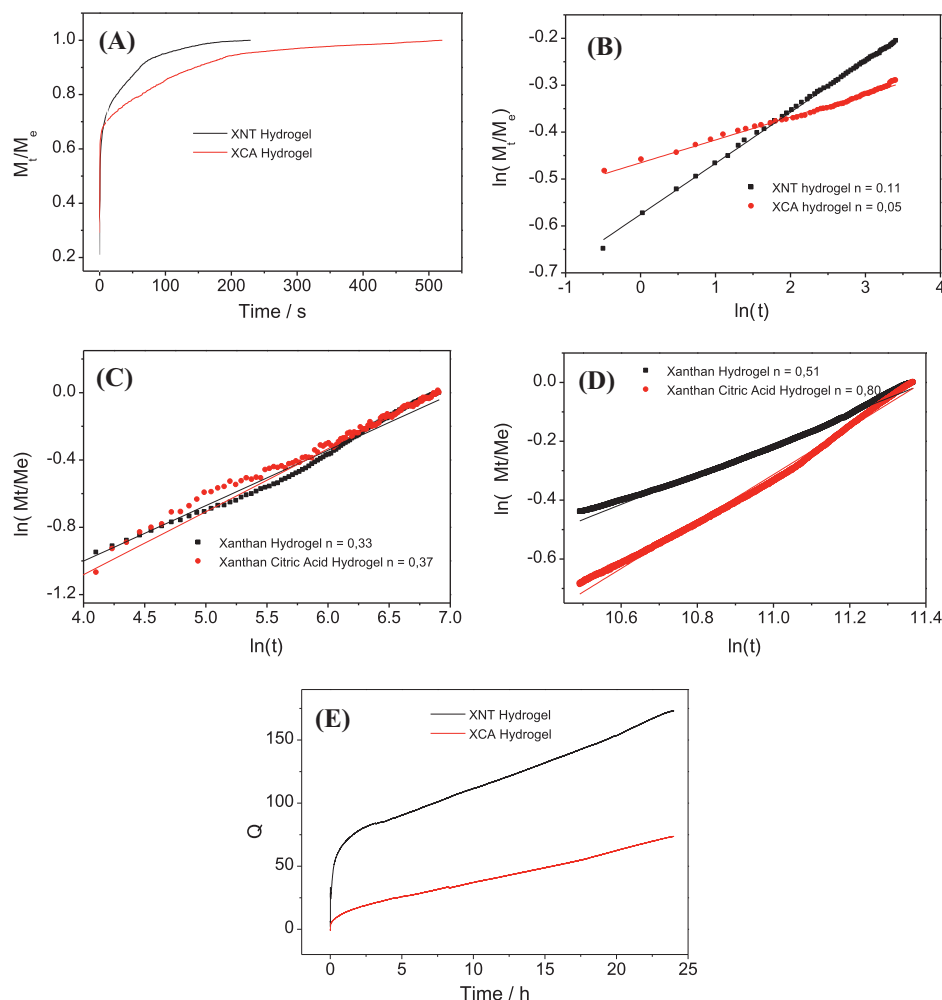


Fig. 3. (A) Variation $M_t/M_e \times t$ curves for absorption of *n*-hexane by hydrogels samples. (B) Linearization of shown curves for *n*-hexane absorption. (C) Linearization of first 1000 s and (D) 10 h until final of curve of water absorption. (E) Variation of xanthan-based hydrogels swelling with the time.

hydrogels), which can be completely deprotonated at $\text{pH} > 6$. Moreover, under basic medium, the unreacted hydroxyl groups are also deprotonated and ester bonds undertake alkaline hydrolysis. Thus, electrostatic repulsion and crosslink disruption favor the increase in swelling ratio (Q/Q_0) observed for hydrogels in basic medium, as show in Fig. 4. XCA hydrogels are more sensitive to pH variation than XNT hydrogels, because they have more crosslinks to be hydrolyzed than XNT hydrogels. At pH 2 and pH 6.5 there is no significant effect of pH on the Q/Q_0 values.

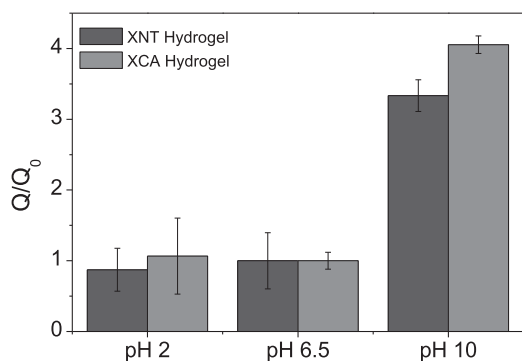


Fig. 4. Effect of pH on the swelling ratio (Q/Q_0) of XNT and XCA hydrogels.

Effects of media pH on pores morphology are exemplified in Fig. 5. At $\text{pH} \sim 10$ the original morphological features changed and the pore size increased significantly, corroborating with the increase in the (Q/Q_0) values observed in Fig. 4. Comparing the images obtained at pH 6.5 with those at pH 2, the pore size decreased, particularly in the XCA hydrogels. Under acidic conditions charges are scarce, favoring pore collapse.

Fig. 6 shows Q/Q_0 values at equilibrium of XCA and XNT hydrogels in the presence of Hofmeister monovalent anions and cations. The hydrogel was exhaustively rinsed with pure water, which reduces counter ions linked to xanthan chains. In general, Q/Q_0 decreased about 20%. A similar behavior was observed for poly(*N*-vinyl-2-pyrrolidone) (Bueno et al., 2009; Takano et al., 1998) or poly(allylamine)hydrochloride and PVA hydrogels (Muta, Miwa, & Satoh, 2001). Fig. 6A shows the Q/Q_0 values determined for XNT and XCA hydrogels in the presence of Hofmeister monovalent anions, namely, F^- , Cl^- and SCN^- , with Na^+ as counter-ion at 1.0 mol L^{-1} and pH about 6.5. Gel shrinking ($Q/Q_0 < 1.0$) was observed for all systems, except for XCA in the presence of SCN^- ions, corroborating with reported data for Hofmeister series effect on hydrogel swelling (Bueno et al., 2009; Takano et al., 1998). Polarizable ions (chaotropes) tend to adsorb on polar surfaces (Blachechen et al., 2012), increasing the charge density and, therefore, promoting electrostatic repulsion. In case of hydrogels, electrostatic repulsion increases Q/Q_0 , what can explain light increase on XCA hydrogel

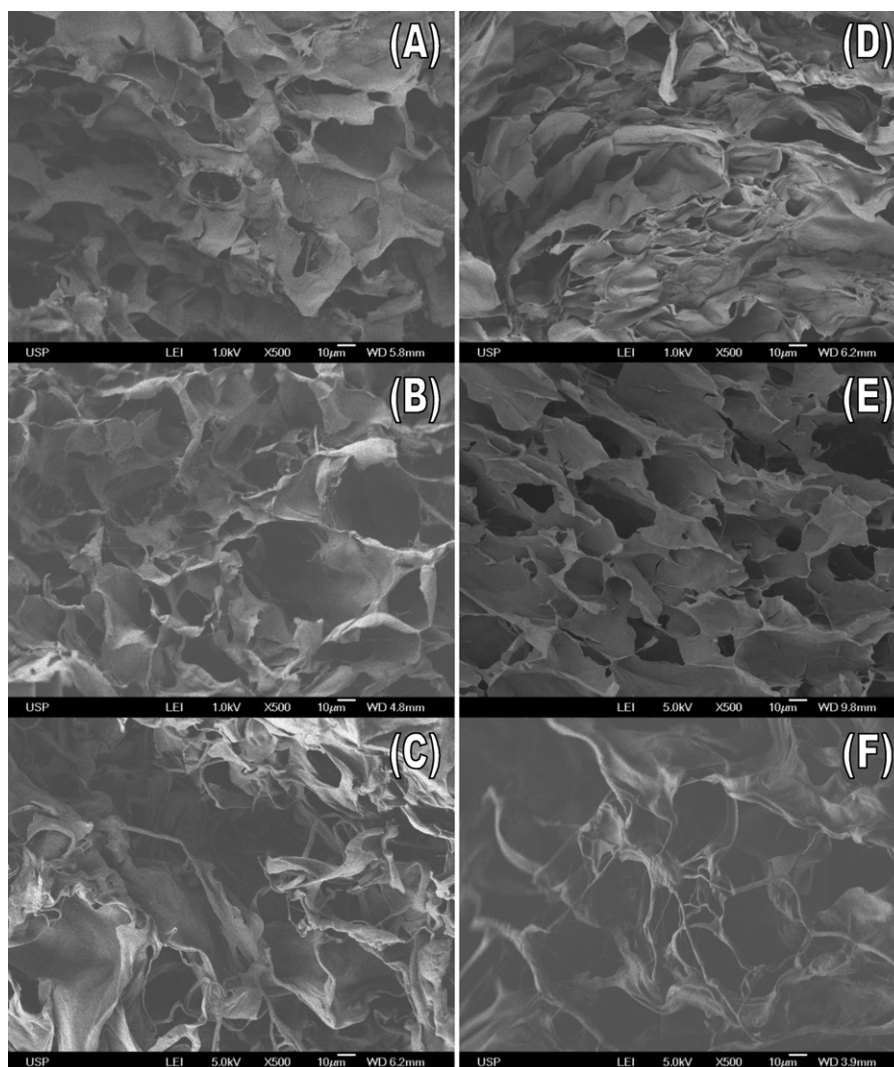


Fig. 5. SEM images of hydrogels. (A), (B) and (C) XNT hydrogel in acid, neutral and basic media, respectively; (D), (E) and (F) XCA hydrogel in acid, neutral and basic media, respectively.

swelling in the presence of SCN^- . In the presence of F^- (kosmotrope), shrinking effects were smaller than expected. One should notice that F^- ions in water are hydrolyzed, generating HF and OH^- ions, which increase the medium pH. In this experiment, NaF induced pH to increase to ~ 9.0 . As observed in Fig. 4, alkaline conditions favor crosslinking disruption and charge density increases; consequently, they increase hydrogel swelling. Therefore, the Q/Q_0 values did not decrease as expected in the presence of F^- because the dehydration was compensated by pore rupture.

The shrinking behavior of XNT and XCA was also investigated in the presence of Li^+ , Na^+ and K^+ , with Cl^- as common counter-ion, at 1.0 mol L^{-1} and pH 6.5, as shown in Fig. 6B. The Q/Q_0 values indicated that XNT hydrogels shrinking was more pronounced than that of XCA hydrogels, especially in the presence of Li^+ (kosmotrope). Interestingly, XCA hydrogels were better swollen in the presence of Li^+ than in pure water. Such behavior might be discussed in the light of specific interaction between Li^+ and solvation layer of xanthan carbonyl or hydroxyl groups. Moreover, XCA hydrogels, which are

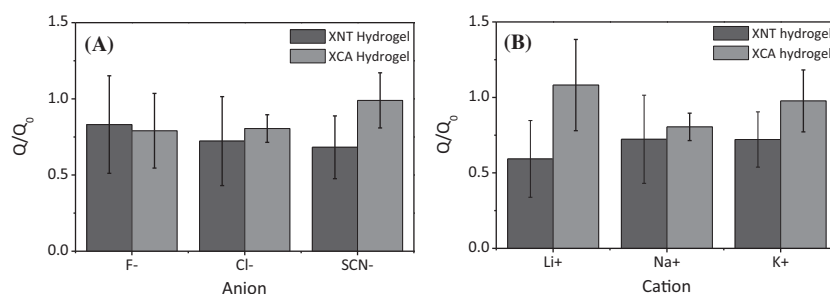


Fig. 6. Effect of Hofmeister series of (A) anions and (B) cations on relative swelling of xanthan hydrogels.

carbonyl rich, are more affected by EPA of water, which increases hydration and consequently, hydrogel swelling. On the other hand, since the carbonyl content in the XNT hydrogels is smaller than in the XCA hydrogels, shrinking behavior of XNT might be better explained by osmotic effects.

4. Conclusion

Xanthan chemical hydrogels can be easily obtained by crosslinking with citric acid, a nontoxic crosslinker, by heating esterification. Crosslinking of xanthan chains in the presence of citric acid led to network with higher crosslinking density. Tensiometry allowed understanding the swelling mechanism of xanthan hydrogels. Initial water uptake mechanism does not depend on hydrogel composition in these cases, and is related to preferential passage of the solvent by interconnected pores without interaction with polymeric chains, as *n*-hexane uptake. Hydrogel swelling, which is the event that follows hydrogel wicking, can be controlled by hydrogel composition, and changes from Fickian (water diffusion does not depend on chains relaxation) to Anomalous (there is interaction between diffusive water and polymeric chains) with the presence of citric acid.

XNT and XCA hydrogels presented high acid resistance, but under alkaline conditions swelling degree increased, especially for XCA samples, due to ester linkages hydrolysis. Such behavior is desirable for the development of pH-controlled drug delivery systems, which protect the drug by preventing its delivery until higher pH environment of the small intestine is reached.

Understanding hydrogel swelling behavior with salts is important for applications involving high ionic strength. Three different effects described hydrogels behavior, depending on the kind of salt and hydrogel. Chaotropes anions, as SCN^- , seem to interact directly with polymeric chains, causing swelling increase, as observed for XCA hydrogels. Kosmotropes cations, as Li^+ , are able to enhance EPA ability of water, increasing stability of carbonyl groups solvation layer and swelling, particularly for hydrogels which are carbonyl rich, as XCA hydrogel. Although kosmotropes anions, as F^- are supposed to present strong shrinking effects on carbonyl rich hydrogels, because they are able to enhance EPD ability of water, destabilizing carbonyl hydration layer, this effect was not observed. The reason is the competition between F^- induced shrinking effect and pH swelling increase effect due to pH increase. Shrinking effects were observed for the other tested ions and XNT hydrogels. Those were related to osmotic effects, observed in the absence of specific interactions between ion and macromolecule or their solvation layer.

Acknowledgement

We thank Brazilian Agency FAPESP (process # 2010/13034-2 and # 2010/51219-5) CAPES Rede Nanobiotec and CNPq for the financial support.

Appendix A. Supplementary data

Supplementary data associated with this article can be found, in the online version, at <http://dx.doi.org/10.1016/j.carbpol.2012.10.062>.

References

Aouada, F. A., Moura, M. R., Silva, W. T. L., Muniz, E. C., & Mattoso, L. H. C. (2011). Preparation and characterization of hydrophilic spectroscopic, and kinetic properties of hydrogels based on polyacrylamide and methylcellulose polysaccharide. *Journal of Applied Polymer Science (Print)*, 120, 3004–3013.

- Bejenariu, A., Popa, M., Picton, L., & Le Cerf, D. (2009). Synthesis of xanthan based hydrogels. Influence of the synthesis parameters on hydrogels behaviour. *Revue Roumaine de Chimie*, 54, 565–569.
- Bejenariu, B., Popa, M., Dulong, V., Picton, L., & Le Cerf, D. (2009). Trisodium trimetaphosphate crosslinked xanthan networks: Synthesis, swelling, loading and releasing behavior. *Polymer Bulletin*, 62, 525–538.
- Bergmann, D., Furth, G., & Mayer, C. (2008). Binding of bivalent cations by xanthan in aqueous solution. *International Journal of Biological Macromolecules*, 43, 245–251.
- Blachechen, L. S., Silva, J. O., Barbosa, L. R. S., Itri, R., & Petri, D. F. S. (2012). Hofmeister effects on the colloidal stability of poly(ethylene glycol)-decorated nanoparticles. *Colloids & Polymer Science*, 290, 1537–1546. <http://dx.doi.org/10.1007/s00396-012-2684-0>
- Bueno, V. B., Cuccovia, I. M., Chaimovich, H., & Catalani, L. H. (2009). PVP superabsorbent nanoparticles. *Colloid and Polymer Science*, 287, 705–713.
- Cacace, M. G., Landau, E. M., & Ramsden, J. J. (1997). The Hofmeister series: Salt and solvent effects on interfacial phenomena. *Quarterly Reviews of Biophysics*, 30, 241–277.
- Candido, J. S., Leita, R. C. F., Ricardo, N. M. P. S., Feitosa, J. P. A., Muniz, E. C., & Rodrigues, F. H. A. (2012). Hydrogels composite of poly(acrylamide-co-acrylate) and rice husk ash. I. Synthesis and characterization. *Journal of Applied Polymer Science (Online)*, 123, 879–887.
- da Cunha, P. L. R., de Paula, R. C. M., & Feitosa, J. P. A. (2009). Polysaccharides from Brazilian biodiversity: An opportunity to change knowledge into economic value. *Quimica Nova*, 32, 649–660.
- Dário, A. F., Hortêncio, L. M. A., Sierakowski, M. R., Queiroz Neto, J. C., & Petri, D. F. S. (2011). The effect of calcium salts on the viscosity and adsorption behavior of xanthan. *Carbohydrate Polymers*, 84, 669–676.
- Dumitriu, S. (2005). *Polysaccharides: Structural diversity and functional versatility*. New York: Marcel Dekker.
- Fredolini, C., Meani, F., Reeder, K. A., Rucker, S., Patanarut, A., Botterell, P. J., et al. (2008). Concentration and preservation of very low abundance biomarkers in urine, such as human growth hormone (hGH), by Cibacron Blue F3G-A loaded hydrogel particles. *Nano Research*, 1, 502–518.
- Galet, L., Patry, S., & Dodds, J. (2010). Determination of the wettability of powders by the Washburn capillary rise method with bed preparation by a centrifugal packing technique. *Journal of Colloid and Interface Science*, 346, 470–475.
- Geckil, H., Xu, F., Zhang, X., Moon, S. J., & Demirci, U. (2010). Engineering hydrogels as extracellular matrix mimics. *Nanomedicine*, 5, 469–484.
- Geremia, R., & Rinaudo, M. (2005). Biosynthesis, structure, and physical properties of some bacterial polysaccharides. In S. Dumitriu (Ed.), *Polysaccharides: Structural diversity and functional versatility*. Marcel Dekker: New York.
- Gulrez, S. K. H., Al-Assaf, S., & Phillips, G. O. (2011). Hydrogels: Methods of preparation, characterization and applications. In A. Carpi (Ed.), *Progress in molecular and environmental bioengineering – From analysis and modeling to technology applications* (pp. 117–150). Rijeka, Croatia: InTech Publisher.
- Hansen, C. M. (2010). The significance of the surface condition in solutions to the diffusion equation: Explaining anomalous sigmoidal, Case II, and Super Case II absorption behavior. *European Polymer Journal*, 46, 651–662.
- Hill, D. J. T., Lim, M. C. H., & Whittaker, A. K. (1999). Water diffusion in hydroxyethyl methacrylate (HEMA)-based hydrogels formed by *g*-radiolysis. *Polymer International*, 48, 1046–1052.
- Hoffman, A. S. (2002). Hydrogels for biomedical applications. *Advanced Drug Delivery Reviews*, 43, 3–12.
- Kacmaz, A., & Gurdag, G. (2006). Swelling behavior of N-t-butylacrylamide copolymer and terpolymers. *Macromolecular Symposia*, 239, 138–151.
- Krongauz, V. V. (2010). Diffusion in polymers dependence on crosslink density. *Journal of Thermal Analysis and Calorimetry*, 102, 435–445.
- Kunz, W., Lo Nostro, P., & Ninham, B. W. (2004). The present state of affairs with Hofmeister effects. *Current Opinion in Colloid & Interface Science*, 9, 1–18.
- Lai, F. K., & Li, H. (2010). Modeling of effect of initial fixed charge density on smart hydrogel response to ionic strength of environmental solution. *Soft Matter*, 6, 311–320.
- Leontidis, E. (2002). Monolayers, bilayers and micelles of zwitterionic lipids as model systems for the study of specific anion effects. *Current Opinion in Colloid & Interface Science*, 7, 81–91.
- Londhe, S., Gattani, S., & Surana, S. (2010). Development of floating drug delivery system with biphasic release for verapamil hydrochloride: In vitro and in vivo evaluation. *Journal of Pharmaceutical Science & Technology*, 2, 361–367.
- Manciu, M., & Ruckenstein, E. (2007). On possible microscopic origins of the swelling of neutral lipid bilayers induced by simple salts. *Journal of Colloid and Interface Science*, 309, 56–67.
- Masoodi, R., & Pillai, K. M. (2010). Darcy's law-based model for wicking in paper-like swelling porous media. *AIChE Journal*, 56, 2257–2267.
- Mudassir, J., Ranjha, N. M., & Sheikh, Z. Z. (2011). Synthesis and Characterization of pH-sensitive pectin/acrylic acid hydrogels for verapamil release study. *Iranian Polymer Journal*, 20, 147–159.
- Muta, H., Miwa, M., & Satoh, M. (2001). Ion-specific swelling of hydrophilic polymer gels. *Polymer*, 42, 6313–6316.
- Muta, H., Kojima, R., Kawauchi, S., Tachibana, A., & Satoh, M. (2001a). Ion-specificity for hydrogen-bonding hydration of polymer: An approach by ab initio molecular orbital calculations. *Journal of Molecular Structure: THEOCHEM*, 536, 219–226.
- Muta, H., Kojima, R., Kawauchi, S., Tachibana, A., & Satoh, M. (2001b). Ion-specificity for hydrogen-bonding hydration of polymer: An approach by ab initio molecular orbital calculations II. *Journal of Molecular Structure: THEOCHEM*, 574, 195–211.
- Muta, H., Kawauchi, S., & Satoh, M. (2003). Ion-specific swelling behavior of uncharged poly(acrylic acid) gel. *Colloid and Polymer Science*, 282, 149–155.

- Muzzarelli, R. A. A. (2009). Chitins and chitosans for the repair of wounded skin, nerve, cartilage and bone. *Carbohydrate Polymers*, 76, 167–182.
- Pal, K., Banthia, A. K., & Majundar, D. K. (2009). Polymeric hydrogels: Characterization and biomedical applications – A mini review. *Designed Monomers & Polymers*, 12, 197–220.
- Peppas, N. A. M. (1986). *Hydrogels in Medicine and Pharmacy Fundamentals*. Boca Raton: CRC Press.
- Petrache, H. I., Zemb, T., Belloni, L., & Parsegian, V. A. (2006). Salt screening and specific ion adsorption determine neutral-lipid membrane interactions. *Proceedings of the National Academy of Sciences of the United States of America*, 103, 7982–7987.
- Reddy, N., & Yang, Y. Q. (2010). Citric acid cross-linking of starch films. *Food Chemistry*, 118, 702–711.
- Rudzinski, W. E., Dave, A. M., Vaishnav, U. H., Kumbar, S. G., Kulkarni, A. R., & Aminabhavi, T. M. (2002). Hydrogels as controlled release devices in agriculture. *Designed Monomers & Polymers*, 5, 39–65.
- Santos, A. P., & Levin, Y. (2011). Ion specificity and the theory of stability of colloidal suspensions. *Physical Review Letters*, 106, 167801 1–167801 4.
- Saunders, B. R., & Vincent, B. (1999). Microgel particles as model colloids: Theory, properties and applications. *Advances in Colloid and Interface Science*, 80, 1–25.
- Shalviri, A., Liu, Q., Abdekhodaie, M. J., & Wu, X. Y. (2010). Novel modified starch–xanthan gum hydrogels for controlled drug delivery: Synthesis and characterization. *Carbohydrate Polymers*, 79, 898–907.
- Solinis, M. A., De la Cruz, Y., Calvo, B., Hernandez, R. M., Gascon, A. R., Goni, I., et al. (2002). Release of salbutamol sulphate and ketoprofen enantiomers from matrices containing HPMC and cellulose derivatives. *Chirality*, 14, 806–813.
- Soppimath, K. S., Aminabhavi, T. M., Dave, A. M., Kumbar, S. G., & Rudzinski, W. E. (2002). Stimulus-responsive “smart” hydrogels as novel drug delivery systems. *Drug Development and Industrial Pharmacy*, 28, 957–974.
- Takano, M., Ogata, K., Kawauchi, S., Satoh, M., & Komiyama, J. (1998). Ion-specific swelling behavior of poly(N-vinyl-2-pyrrolidone) gel: Correlations with water hydrogen bond and non-freezable water. *Polymer Gels and Networks*, 6, 217–232.
- Thakur, A., Wanchoo, R. K., & Singh, P. (2011). Structural parameters and swelling behavior of pH sensitive poly(acrylamide-co-acrylic acid) hydrogels. *Chemical and Biochemical Engineering Quarterly*, 25, 181–194.
- Thomas, N. L., & Windle, A. H. (1982). A theory of Case-II diffusion. *Polymer*, 23, 529–542.
- Tinland, B., & Rinaudo, M. (1989). Dependence of the stiffness of the xanthan chain on the external salt concentration. *Macromolecules*, 22, 1863–1865.
- Veiga-Santos, P., Oliveira, L. M., Cereda, M. P., Alves, A. J., & Scamparini, A. R. P. (2005). Mechanical properties, hydrophilicity and water activity of starch–gum films: Effect of additives and deacetylated xanthan gum. *Food Hydrocolloids*, 19, 341–349.
- Wisniewski, S., & Kim, S. W. (1980). Permeation of water-soluble solutes through poly(2-hydroxyethyl methacrylate) and poly(2-hydroxyethyl methacrylate) crosslinked with ethylene glycol dimethacrylate. *Journal of Membrane Science*, 6, 299–308.
- Wu, Y., Joseph, S., & Aluru, N. R. (2009). Effect of cross-linking on the diffusion of water, ions, and small molecules in hydrogels. *Journal of Physical Chemistry B*, 113, 3512–3520.
- Yang, C. Q., Wang, X., & Kang, I. (1997). Ester cross-linking of cotton fabric by polymeric carboxylic acids and citric acid. *Textile Research Journal*, 67, 334–342.
- Zhang, Y., & Cremer, P. S. (2006). Interactions between macromolecules and ions: The Hofmeister series. *Current Opinion in Chemical Biology*, 10, 658–663.
- Zhang, Y., Furry, S., Bergbreiter, D. E., & Cremer, P. S. (2005). Specific ion effects on the water solubility of macromolecules: PNIPAM and the Hofmeister series. *Journal of the American Chemical Society*, 127, 14505–14510.
- Zuidema, J. M., Pap, M. M., Jaroch, D. B., Morrison, F. A., & Gilbert, R. J. (2011). Fabrication and characterization of tunable polysaccharide hydrogel blends for neural repair. *Acta Biomaterialia*, 7, 1634–1643.